

# Southern Ocean source of $^{14}\text{C}$ -depleted carbon in the North Pacific Ocean during the last deglaciation

C. Basak<sup>1\*</sup>, E. E. Martin<sup>1</sup>, K. Horikawa<sup>1</sup> and T. M. Marchitto<sup>2</sup>

**During the last deglaciation, atmospheric carbon dioxide concentrations rose at the same time that the  $\Delta^{14}\text{C}$  of that  $\text{CO}_2$  fell. This has been attributed to the release of  $^{14}\text{C}$ -depleted carbon dioxide from the deep ocean<sup>1</sup>, possibly vented through the Southern Ocean<sup>2–5</sup>. Recently, a sediment record from the eastern North Pacific Ocean spanning the last deglaciation was interpreted to reflect transport of such radiocarbon-depleted  $\text{CO}_2$  from the Southern Ocean through Antarctic Intermediate Water<sup>2</sup>. However, the suggestion that the record reflects intermediate water derived from the Southern Ocean remains controversial. Here we assess the source of the deglacial intermediate water by measuring the neodymium isotopes of fossil fish teeth/debris from the same eastern North Pacific core used in the earlier study<sup>2</sup>. The isotopic signature of a water mass, which is captured in the fossil fish teeth, reflects the location in which it formed. Our data exhibit a clear shift in the neodymium isotope values towards Southern Ocean values about 18,000 years ago, coinciding with the negative  $\Delta^{14}\text{C}$  excursion. We conclude that these data support a Southern Ocean source for the deglacial radiocarbon-depleted  $\text{CO}_2$  detected in the eastern North Pacific.**

Negative radiocarbon excursions<sup>2,6</sup> observed in the eastern tropical Pacific Ocean are contemporaneous with increased upwelling in the Southern Ocean<sup>7</sup> and onset of warming and rising  $\text{CO}_2$  detected in Antarctic ice cores<sup>8</sup>, highlighting a possible cause and effect relationship between circulation in the Southern Hemisphere and radiocarbon in the eastern tropical Pacific Ocean. Despite these observations, there is no direct evidence that this older water was sourced from the Southern Ocean. An alternative possible source is the high-latitude North Pacific. There is no clear way to distinguish between northern and southern routing on the basis of  $\Delta^{14}\text{C}$ ,  $\delta^{13}\text{C}$  or  $\delta^{18}\text{O}$  because similar oceanic and atmospheric processes could theoretically act to modify the isotopic characteristics of either endmember water mass. In contrast, Nd isotopes in fossil fish teeth/debris are considered quasiconservative tracers of water mass (Supplementary Information), meaning that major water masses carry distinct Nd isotopic ratios (reported here as  $\epsilon_{\text{Nd}}$ ) that are generally altered only by mixing, although modification by local weathering inputs is possible.

Our core location and depth is at present situated at the boundary between Equatorial Intermediate Water (EqIW) (a mixture of Antarctic Intermediate Water (AAIW) and upwelled Pacific Deep Water (PDW))<sup>9</sup>, and North Pacific Intermediate Water (NPIW) within the east Pacific shadow zone (Fig. 1; Supplementary Information). Limited data for PDW from the deep tropical waters indicate very little variation in  $\epsilon_{\text{Nd}}$  since the Last Glacial Maximum<sup>10</sup> (LGM). Thus, the  $\epsilon_{\text{Nd}}$  value at Baja is

largely controlled by the relative contributions of NPIW (higher values) and AAIW (lower values), with AAIW values modified during transit from the Southern Ocean through the Papua New Guinea region.

We report a Nd isotope time series for the past 38 kyr from core MV99-MC19/GC31/PC08 near southern Baja California using the same samples and age model as Marchitto *et al.*<sup>2</sup> to distinguish between potential northern and southern sources for the old,  $^{14}\text{C}$ -depleted water detected during the last deglaciation. Our record illustrates variations in  $\epsilon_{\text{Nd}}$  values from  $-0.3$  to  $-3.0$ . Pre-LGM (before 21 kyr BP)  $\epsilon_{\text{Nd}}$  values range between  $-1$  and  $-2.5$ , with values around  $-1$  during the LGM. A prominent negative excursion to approximately  $-3.0$  occurs at the beginning of the deglaciation, with a subsequent increase to  $-1.7$  during the later half of Heinrich Stadial 1 (HS1). Nd isotopic values continue to increase into the Bølling–Allerød (B–A) warm interval, where they plateau at  $\sim -1.4$ . There is limited data during the cold Younger Dryas (YD) interval; however, there is a hint of a minor negative  $\epsilon_{\text{Nd}}$  excursion during the YD followed by a positive excursion and values ranging from  $-0.3$  to  $-1.6$  in the Holocene epoch. There is some structure in the Holocene record, but the mean  $\epsilon_{\text{Nd}}$  value is comparable to LGM values and tends to be higher than pre-LGM values.

In general, modern AAIW  $\epsilon_{\text{Nd}}$  values are  $\sim -6$  to  $-8\epsilon_{\text{Nd}}$  units and NPIW values are  $\sim 0$  to  $-4\epsilon_{\text{Nd}}$  units (ref. 11 and references therein; Supplementary Information). Thus, the overall  $-0.3$  to  $-3.0$  range in  $\epsilon_{\text{Nd}}$  values observed in our data would seem to represent waters dominantly sourced from the North Pacific throughout the past 38 kyr. However, the Nd isotope signature of southern-sourced AAIW is modified during its transit through the Pacific in the region of Papua New Guinea because of interactions with volcanic inputs that introduce much higher Nd isotopic ratios ( $\epsilon_{\text{Nd}} \sim +7$ ; ref. 12). As a result, the measured  $\epsilon_{\text{Nd}}$  value of this modified AAIW is  $\sim -2.8$  (ref. 12; Supplementary Information), and it is this water that flows eastward along the Equator to influence EqIW. In addition, our youngest  $\epsilon_{\text{Nd}}$  value of  $-1.5$  may be taken as a minimum value for modern NPIW in this region based on the most conservative scenario that the site is at present bathed by pure NPIW.

In the absence of any high-resolution  $\epsilon_{\text{Nd}}$  reconstructions from the AAIW and NPIW source regions, we begin with the assumption that the endmember compositions of these two water masses have remained relatively constant since the LGM. In the context of constant endmembers,  $\epsilon_{\text{Nd}}$  excursions to more radiogenic values represent an increased flux of NPIW (or less AAIW), whereas excursions towards less radiogenic values record an increased flux of AAIW (or less NPIW). Following this logic, the pre-LGM period (before 21 kyr BP) in our record indicates a mixture of NPIW and

<sup>1</sup>Department of Geological Sciences, University of Florida, Gainesville, Florida 32611, USA, <sup>2</sup>Department of Geological Sciences and Institute of Arctic and Alpine Research, University of Colorado, Boulder, Colorado 80309, USA. \*e-mail: basakc1@ufl.edu.

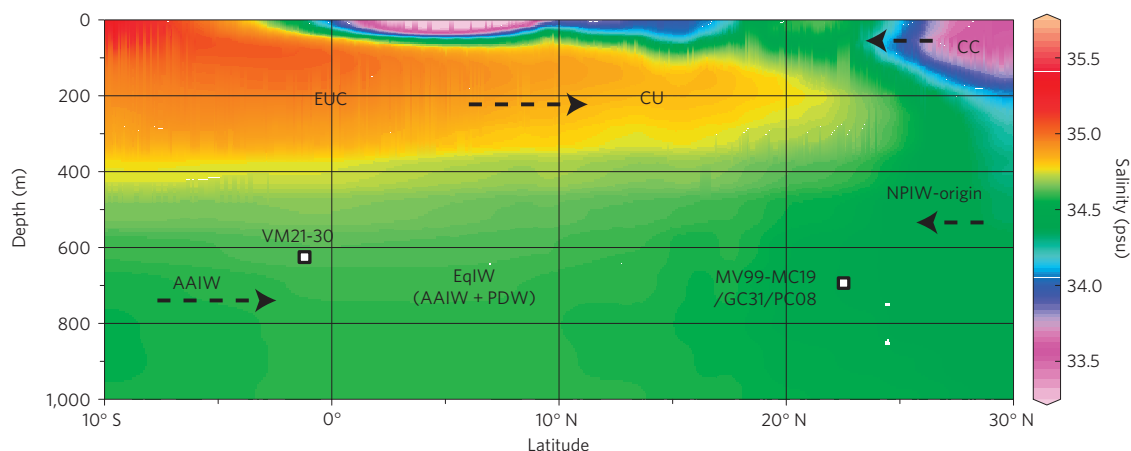


**Figure 1 | Modern hydrography.** Depth profile of annual mean salinity along the continental margin of the eastern North Pacific. Cores MV99-MC19/GC31/PC08 (23.5° N, 111.6° W; ref. 2) and VM21-30 (1° S, eastern equatorial Pacific; ref. 6) are bathed by EqIW, which is largely a combination of NPIW, AAIW and PDW. CC: California Current; CU: California Undercurrent; EUC: Equatorial Undercurrent.

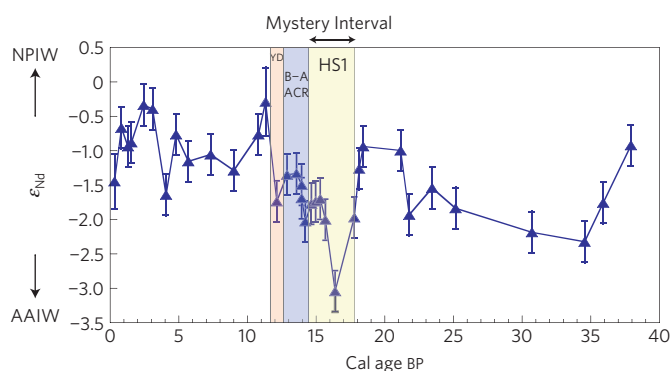


**Figure 2 |  $\epsilon_{\text{Nd}}$  record from Baja California for the past 38 kyr.**  $\epsilon_{\text{Nd}}$  of fossil fish teeth/debris plotted against calendar age highlights water mass variations at the Baja site for the past 38 kyr ( $\epsilon_{\text{Nd}} = ((^{143}\text{Nd}/^{144}\text{Nd})_{\text{measured}} / (^{143}\text{Nd}/^{144}\text{Nd})_{\text{CHUR}} - 1) \times 10^4$ ). The vertical error bars represent long-term external reproducibility of the JNdi-1 standard (0.3 $\epsilon_{\text{Nd}}$  units) except for samples with a higher internal error. The yellow, blue and orange shaded areas indicate HS1, B-A and YD climate episodes. The period between 14.5 and 17.5 kyr BP is referred to as the 'Mystery Interval'.

AAIW, with a relatively decreased component of AAIW during the LGM, similar to Holocene values (Fig. 2). AAIW intensified during the deglaciation, comprising most of the water mass during the early part of the HS1 event, then decreased during the B-A warming period and might have increased slightly again during the YD. Post YD the region was once again dominated by NPIW.

The timing of major fluctuations in AAIW interpreted from Nd isotopes is broadly in agreement with the idea of depleted  $^{14}\text{C}$  originating in the Southern Ocean (Fig. 3b,c). The deglacial decrease in  $\epsilon_{\text{Nd}}$  values around 18 kyr BP probably represents the first pulse of AAIW into the eastern North Pacific as the Southern Ocean recovered from surface stratification<sup>4,5</sup> and/or extensive sea-ice coverage<sup>3</sup> during the LGM. The timing of this pulse defined by Nd isotopes coincides with a negative  $\delta^{13}\text{C}$  excursion of thermocline-dwelling foraminifera *Neogloboquadrina dutertrei* in the eastern equatorial Pacific<sup>13,14</sup> also interpreted to indicate an influx of older water from the Southern Ocean (Fig. 3d). In the Southern Ocean higher productivity indicated by an increased opal flux near Antarctica also supports increased upwelling of nutrient-rich abyssal water and hence more AAIW activity<sup>7</sup> at this time (Fig. 3e). Evidence of

increased deglacial AAIW has also been reported from Nd isotopic records in the Atlantic<sup>15</sup>.

Comparison of Northern Hemisphere<sup>16</sup> and Southern Hemisphere<sup>8</sup> ice-core temperatures indicates that deglacial warming in the Southern Ocean preceded deglaciation in the high-latitude Northern Hemisphere (Fig. 3a). Early warming in the Southern Hemisphere and invigorated AAIW formation are well known<sup>2,17,18</sup>. In contrast, the deep and shallow Northern Pacific did not start responding to deglaciation until the beginning of the B-A period<sup>19</sup> (~14.8 kyr BP), although localized intermediate water formation during HS1 in the western North Pacific has recently been reported<sup>20</sup>. Therefore, temporal differences in the deglacial history between the Northern and Southern hemispheres also imply that the Nd isotopic excursion at ~18 kyr was controlled by intermediate water mass readjustment in the Southern Hemisphere.

The deep ocean represents the most likely storage area for old carbon during the last glaciation because of the proposed mechanism of formation and the volume of the old carbon reservoir<sup>1,21</sup>. Our  $\epsilon_{\text{Nd}}$  data imply that the old carbon reported from the Baja site<sup>2</sup> was sourced from the Southern Ocean through AAIW that was modified in the equatorial Pacific. A recent study indicates<sup>22</sup> no evidence for deglacial old  $^{14}\text{C}$  in intermediate waters off Chile, close to one of the main regions of AAIW formation today. Part of this AAIW takes a complicated route in the South Pacific before reaching the Baja site (Supplementary Information). Another portion of this AAIW passes from the southeastern Pacific, through Drake Passage<sup>23</sup> and circumnavigates Antarctica where it could have picked up old carbon from the deep southern abyss before circulating back into the Indian and Pacific oceans. The Chilean site<sup>22</sup> may be too close to the region of active AAIW formation to have been influenced by AAIW that acquired older carbon during its journey around Antarctica. Recent evidence of radiocarbon-depleted AAIW reported from the tropical South Atlantic off Brazil during the HS1 and YD intervals<sup>24</sup> and from the deep Southern Ocean<sup>25</sup> during the last glacial period is consistent with acquisition of old abyssal carbon east of Drake Passage.

Half way through the HS1 event  $\epsilon_{\text{Nd}}$  values in the Baja record become more positive in a pattern that does not match the Baja  $\Delta^{14}\text{C}$  record. The  $\Delta^{14}\text{C}$  record depicts a strong influence of aged water until the beginning of the B-A period (Fig. 3c), whereas the  $\epsilon_{\text{Nd}}$  record illustrates increasing values during the later half of HS1, which could be interpreted as decreasing AAIW. However, no other lines of evidence support diminished AAIW at this time<sup>7,8,13</sup> (Fig. 3). Alternatively, an increased NPIW flux could potentially explain the observed discrepancy during the mid HS1. Although the western

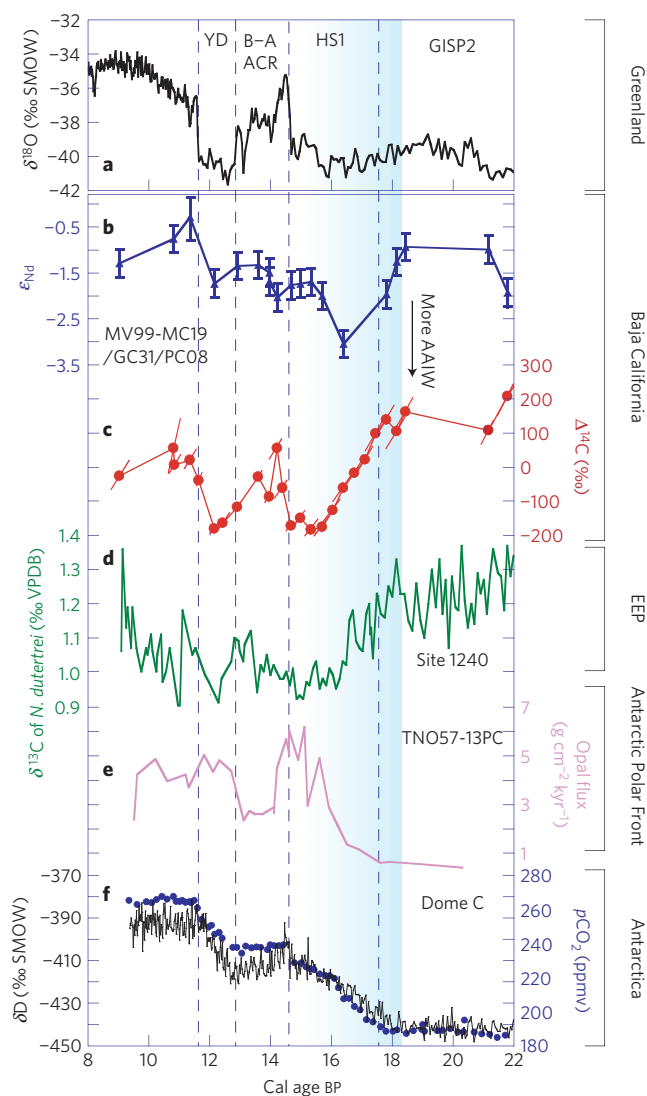


**Figure 3 | Meridional multi-proxy responses to the last deglaciation (8–22 kyr BP).** **a**, Greenland ice-core temperatures<sup>16</sup>. **b**,  $\epsilon_{\text{Nd}}$  from MV99-MC19/GC31/PC08. **c**,  $\Delta^{14}\text{C}$  from MV99-MC19/GC31/PC08 (ref. 2), error bars are based on compounded uncertainties in radiocarbon ages and calendar ages. **d**,  $\delta^{13}\text{C}$  of thermocline-dwelling foraminifera *Neogloboquadrina dutertrei* in the eastern equatorial Pacific (EEP) (ref. 14). **e**, Opal flux data from the Antarctic Polar Front<sup>7</sup>. **f**, Atmospheric  $\text{CO}_2$  (blue circles) and ice-core deuterium ( $\delta\text{D}$ ) temperature proxy (black) from Antarctic Dome C (ref. 8) placed on the GISP 2 timescale<sup>2</sup>. The blue shaded area highlights the initial deglaciation.

North Pacific is known to be a region of active intermediate–deep water formation during HS1, these waters were relatively enriched in  $^{14}\text{C}$  and do not seem to have reached the eastern Pacific<sup>20</sup>. In the absence of any compelling evidence in favour of diminished AAIW or increased NPIW, we must appeal to modified endmember  $\epsilon_{\text{Nd}}$  values of AAIW or NPIW to explain the decoupling between  $\Delta^{14}\text{C}$  and  $\epsilon_{\text{Nd}}$ . Given that  $\epsilon_{\text{Nd}}$  values suggest the water at the Baja site is dominated by AAIW by mid HS1, we focus on this endmember. Changes in weathering in the Papua New Guinea region, possibly due to a southward shift of the intertropical convergence zone<sup>26</sup> and increased rainfall around Papua New Guinea during deglaciation, could have introduced more positive Papua New Guinea-type  $\epsilon_{\text{Nd}}$  values to AAIW.

Changes in  $\epsilon_{\text{Nd}}$  during the B–A and YD are more subtle but seem to be consistent with anticipated variations in NPIW and

AAIW. During B–A opal flux data from the Southern Ocean indicate reduced nutrient upwelling and AAIW formation<sup>7</sup>. A relative increase in the proportion of NPIW versus AAIW during the B–A period is consistent with the small increase observed in  $\epsilon_{\text{Nd}}$  at the Baja site. A minor negative  $\epsilon_{\text{Nd}}$  excursion (albeit a one-point low) during the YD is consistent with rejuvenation of AAIW in accordance with  $\Delta^{14}\text{C}$  and other indicators of increased AAIW from the Southern Ocean (Fig. 3b,c). Post YD values are comparable to LGM values, reflecting increased influence of NPIW during the Holocene. This scenario is consistent with rearrangements in Holocene deep and intermediate circulation patterns leading to a modern system that is dominated by NPIW at this site.

Evidence of old carbon at intermediate depths in the eastern North Pacific has been one of the most intriguing palaeoceanographic findings establishing the mechanism of atmospheric  $\text{CO}_2$  leakage at the end of the last glaciation. Direct and indirect evidence in favour of an old carbon reservoir and increased AAIW have been reported from the Southern Ocean<sup>7,13,25</sup>, but there is no direct proof that these Southern waters reached the tropical North Pacific during deglaciation. This coupled study of  $\epsilon_{\text{Nd}}$  and  $\Delta^{14}\text{C}$  reports variations in the relative dominance of more radiogenic NPIW and less radiogenic AAIW over the past 38 kyr and supports the concept of an increased contribution of AAIW at the beginning of the deglaciation, suggesting that the old carbon was transported from the deep southern abyss to the shallow tropics through AAIW.

## Methods

Fossil fish teeth/debris were handpicked from the  $>63\ \mu\text{m}$  fraction of sieved sediments from core MV99-MC19/GC31/PC08 off Baja California. Picked fossil fish teeth/debris were dissolved in a 1:1 mixture of optima grade  $\text{HNO}_3$  and HCl in preparation for column chemistry. A primary column with Mitsubishi resin and 1.6N HCl as an eluent was used to separate bulk rare earth elements. Nd was then isolated by passing the rare earth element aliquot through Ln-spec resin with 0.25N  $\text{HNO}_3$  as an eluent. Procedural blanks were 14 pg Nd.

Nd isotopes were analysed on a Nu Plasma multi-collector inductively coupled plasma mass spectrometer at the University of Florida. Nd aliquots from column chemistry were dried and redissolved in 2%  $\text{HNO}_3$  before aspiration using a DSN-100 nebulizer. Pre-amplifier gain calibrations were run at the beginning of each analytical session. All Nd isotope data reported in this study were analysed using a time-resolved analysis method<sup>27</sup>. Before sample introduction a baseline was measured for 30 s. Data were acquired in a series of 0.2 s integrations over 1–3 min. All reported  $^{143}\text{Nd}/^{144}\text{Nd}$  ratios were corrected for mass fractionation using  $^{146}\text{Nd}/^{144}\text{Nd} = 0.7219$ . International standard JNdi-1 was analysed between every 5 and 6 unknown samples and the average of these standard runs was compared with a long-term TIMS JNdi-1 value of  $0.512103 \pm 0.000014$  to determine a correction factor for each of the samples analysed on that day. The long-term  $2\sigma$  external reproducibility of JNdi-1 analyses on the Nu of 0.000014 ( $0.3\epsilon_{\text{Nd}}$  units) has been applied to all samples unless the internal error was larger.

Received 19 May 2010; accepted 21 September 2010; published online 24 October 2010

## References

- Broecker, W. & Barker, S. A 190‰ drop in atmosphere's  $\Delta^{14}\text{C}$  during the 'Mystery Interval' (17.5 to 14.5 kyr). *Earth Planet. Sci. Lett.* **256**, 90–99 (2007).
- Marchitto, T. M., Lehman, S. J., Ortiz, J. D., Fluckiger, J. & van Geen, A. Marine radiocarbon evidence for the mechanism of deglacial atmospheric  $\text{CO}_2$  rise. *Science* **316**, 1456–1459 (2007).
- Stephens, B. B. & Keeling, R. F. The influence of Antarctic sea ice on glacial–interglacial  $\text{CO}_2$  variations. *Nature* **404**, 171–174 (2000).
- Francois, R. *et al.* Contribution of Southern Ocean surface-water stratification to low atmospheric  $\text{CO}_2$  concentrations during the last glacial period. *Nature* **389**, 929–935 (1997).
- Sigman, D. M. & Boyle, E. A. Glacial/interglacial variations in atmospheric carbon dioxide. *Nature* **407**, 859–869 (2000).
- Stott, L., Southon, J., Timmermann, A. & Koutavas, A. Radiocarbon age anomaly at intermediate water depth in the Pacific Ocean during the last deglaciation. *Paleoceanography* **24**, PA2223 (2009).
- Anderson, R. F. *et al.* Wind-driven upwelling in the southern ocean and the deglacial rise in atmospheric  $\text{CO}_2$ . *Science* **323**, 1443–1448 (2009).
- Monnin, E. *et al.* Atmospheric  $\text{CO}_2$  concentrations over the last glacial termination. *Science* **291**, 112–114 (2001).

9. Bostock, H. C., Opdyke, B. N. & Williams, M. J. M. Characterizing the intermediate depth waters of the Pacific Ocean using  $\delta^{13}\text{C}$  and other geochemical tracers. *Deep-Sea Res. Part I* **57**, 847–859 (2010).
10. Marchitto, T. M., Lynch-Stieglitz, J. & Hemming, S. R. Deep Pacific  $\text{CaCO}_3$  compensation and glacial–interglacial atmospheric  $\text{CO}_2$ . *Earth Planet. Sci. Lett.* **231**, 317–336 (2005).
11. Goldstein, S. L. & Hemming, S. H. in *Treatise on Geochemistry* (ed. Elderfield, H.) 453–489 (Elsevier, 2003).
12. Lacan, F. & Jeandel, C. Tracing Papua New Guinea imprint on the central Equatorial Pacific Ocean using neodymium isotopic compositions and rare earth element patterns. *Earth Planet. Sci. Lett.* **186**, 497–512 (2001).
13. Spero, H. J. & Lea, D. W. The cause of carbon isotope minimum events on glacial terminations. *Science* **296**, 522–525 (2002).
14. Pena, L. D., Cacho, I., Ferretti, P. & Hall, M. A. El Niño—Southern Oscillation—like variability during glacial terminations and interlatitudinal teleconnections. *Paleoceanography* **23**, PA3101 (2008).
15. Pahnke, K., Goldstein, S. L. & Hemming, S. R. Abrupt changes in Antarctic intermediate water circulation over the past 25,000 years. *Nature Geosci.* **1**, 870–874 (2008).
16. Grootes, P. & Stuiver, M. Oxygen 18/16 variability in Greenland snow and ice with  $10^{-3}$  to  $10^5$  year time resolution. *J. Geophys. Res.* **102**, 26455–26470 (1997).
17. Stott, L., Timmermann, A. & Thunell, R. Southern hemisphere and deep-sea warming led deglacial atmospheric  $\text{CO}_2$  rise and tropical warming. *Science* **318**, 435–438 (2007).
18. Toggweiler, J. R., Russell, J. L. & Carson, S. R. Midlatitude westerlies, atmospheric  $\text{CO}_2$ , and climate change during the ice ages. *Paleoceanography* **21**, PA2005 (2006).
19. Galbraith, E. D. *et al.* Carbon dioxide release from the North Pacific abyss during the last deglaciation. *Nature* **449**, 890–893 (2007).
20. Okazaki, Y. *et al.* Deepwater formation in the North Pacific during the last glacial termination. *Science* **329**, 200–204 (2010).
21. Broecker, W. The mysterious  $^{14}\text{C}$  decline. *Radiocarbon* **51**, 109–119 (2009).
22. De Pol-Holz, R., Keigwin, L., Southon, J., Hebbeln, D. & Mohtadi, M. No signature of abyssal carbon in intermediate waters off Chile during deglaciation. *Nature Geosci.* **3**, 192–195 (2010).
23. Talley, L.D. in *Mechanisms of Global Climate Change at Millennial Time Scales* (eds Clark, P. U., Webb, R. S. & Keigwin, L. D.) 1–22 (Geophys. Mono, 1999).
24. Mangini, A. *et al.* Deep sea corals off Brazil verify a poorly ventilated Southern Pacific Ocean during H2, H1 and the Younger Dryas. *Earth Planet. Sci. Lett.* **293**, 269–276 (2010).
25. Skinner, L. C., Fallon, S., Waelbroeck, C., Michel, E. & Barker, S. Ventilation of the deep southern ocean and deglacial  $\text{CO}_2$  rise. *Science* **328**, 1147–1151 (2010).
26. Krebs, U. & Timmermann, A. Tropical air–sea interactions accelerate the recovery of the atlantic meridional overturning circulation after a major shutdown. *J. Clim.* **20**, 4940–4956 (2007).
27. Kamenov, G., Perfit, M., Mueller, P. A. & Jonasson, I. R. Controls on magmatism in an island arc environment: Study of lavas and sub-arc xenoliths from the Tabar–Lihir–Tanga–Feni island chain, Papua New Guinea. *Contrib. Mineral. Petrol.* **155**, 635–656 (2008).

### Acknowledgements

We thank G. Kamenov for technical support regarding Nd isotope analyses on the Nu Plasma multi-collector inductively coupled plasma mass spectrometer at the University of Florida as well as D. Hodell and D. Newkirk for scientific discussions. The manuscript benefited from comments by A. Piotrowski. We also thank A. van Geen for access to core samples. Core retrieval was supported by NSF grant OCE 98-09026 to A. van Geen and Y. Zheng. Financial support for the research was provided by NSF grant OCE-0623393 to E.E.M. Partial support for this research was also provided by GSA Graduate Student Research grant to C.B.

### Author contributions

C.B. and E.E.M. conceived the study. C.B. analysed the Nd isotope data and wrote the paper with the help of all of the co-authors. E.E.M., K.H. and T.M.M. supplied ideas that shaped the final version. All authors contributed towards writing the manuscript.

### Additional information

The authors declare no competing financial interests. Supplementary information accompanies this paper on [www.nature.com/naturegeoscience](http://www.nature.com/naturegeoscience). Reprints and permissions information is available online at <http://npg.nature.com/reprintsandpermissions>. Correspondence and requests for materials should be addressed to C.B.